mention here that the radiation term in the LHS of (1) is linearised in the finite-difference formulation, whereas the present method does not require this linearisation. Minor improvements have however been incorporated in the program. For example, the resulting tridiagonal matrix is solved using the Thomas algorithm. For the sake of comparison, the following values are chosen in both the numerical analyses: $P = 5$, $l = 10$, step size 20 and identical initial temperature profile. It is observed that both the programs need almost the same computer memory, but the CPU time in the present method and the finite-difference method is 0.733 and 1.294 s, respectively on CYBER 170/730 computer. Therefore the present method is economical as compared to the finite-difference method. This shows that it is convenient to use the Runge–Kutta method in conjunction with an iterative scheme to solve nonlinear integro-differential equations.

REFERENCES

1. R. C. Mehta, Heat transfer analysis of hollow cathode, *Proc. 17th Int. Electric Propulsion Conference* (JSASS/AIAA/DGLR), Tokyo (1985).
2. H. C. Hottel, Geometrical problems in radiant heat transfer, *Heat Transfer Lecture*, Vol. II, NEPA-979 IER-13. Fairchild Corporation, Oak Ridge, Tennessee (1949).
3. R. Siegel and E. G. Keshock, Wall temperatures in a tube with forced convection, internal radiation exchange, and axial wall heat conduction, NASA TND-2116 (1964).
4. R. Siegel, Private communication, NASA Lewis Research Center, Cleveland, Ohio (May 1981).
5. R. Siegel and J. R. Howell, *Thermal Radiation Heat Transfer*. McGraw-Hill, New York (1972).
6. C. E. Froberg, *Introduction to Numerical Analysis*. Addison–Wesley, New York (1966).

Int. J. Heat Mass Transfer. Vol. 28, No. 11, pp. 2171–2174, 1985
Printed in Great Britain

0017-9310/85 $3.00 + 0.00
Pergamon Press Ltd.

Finite-difference and improved perturbation solutions for free convection on a vertical cylinder embedded in a saturated porous medium

M. KUMARI, I. POP* and G. NATH†
Department of Applied Mathematics, Indian Institute of Science, Bangalore 560 012, India

(*Received* 29 *January* 1985)

1. INTRODUCTION

THE INVESTIGATION of free convection along a vertical cylinder embedded in a porous medium is of renewed interest in connection with geophysical and engineering applications. The solution of this problem within the framework of boundary-layer approximations has been obtained by Minkowycz and Cheng [1] using the local nonsimilarity method proposed by Sparrow *et al.* [2]. However, this method, which is currently very popular, has its own drawbacks as the derivatives of certain terms are discarded in order to reduce the partial differential equations to ordinary differential equations.

The object of the present paper is to give a more accurate numerical solution of the free convection boundary layer along an isothermal, thin vertical cylinder embedded in a saturated porous medium. In this respect we shall use a new implicit finite-difference scheme developed by Keller [3], and Keller and Cebeci [4] as well as the method of extended perturbation series which is similar to one devised by Aziz and Na [5] for the case of natural convection along an isothermal, thin vertical cylinder immersed in a Newtonian fluid. The specific approach is to extend the series, in terms of the transverse curvature ξ, to five terms and then apply the Shanks [6] transformation twice.

2. GOVERNING EQUATIONS

Let us consider a thin vertical cylinder of radius r_0 maintained at a uniform temperature T_w and embedded in a saturated porous medium with constant physical properties. The radial coordinate r is measured from the axis of the cylinder while the axial coordinate x is measured vertically upward such that $x = 0$ corresponds to the leading edge where the boundary-layer thickness is zero.

Based on Darcy's law and the usual Boussinesq model, the boundary-layer equations, following Minkowycz and Cheng [1], are

$$\frac{\partial}{\partial x}(ru) + \frac{\partial}{\partial r}(rv) = 0 \tag{1}$$

$$u = \frac{\rho_\infty g\beta K}{\mu}(T - T_\infty) \tag{2}$$

$$u\frac{\partial T}{\partial x} + v\frac{\partial T}{\partial r} = \frac{\alpha}{r}\frac{\partial}{\partial r}\left(r\frac{\partial T}{\partial r}\right) \tag{3}$$

with the boundary conditions

$$\begin{aligned} &v = 0, \quad T = T_w \quad \text{on} \quad r = r_0 \\ &u = 0, \quad T = T_\infty \quad \text{as} \quad r \to \infty. \end{aligned} \tag{4}$$

Applying the following transformations

$$\begin{aligned} \psi &= \alpha r(Ra_x)^{1/2}F(\xi,\eta), \\ ru &= \partial\psi/\partial r, \\ rv &= -\partial\psi/\partial x \\ \xi &= (2x/r_0)(Ra_x)^{-1/2}, \\ \eta &= (Ra_x)^{1/2}(r^2 - r_0^2)/(2xr_0) \\ \theta(\xi,\eta) &= (T - T_\infty)/(T_w - T_\infty), \\ Ra_x &= \rho_\infty g\beta Kx(T_w - T_\infty)/(\mu\alpha) \end{aligned} \tag{5}$$

to equations (1)–(3), we find that (1) is identically satisfied and (2) and (3) reduce to

$$\theta = F' \tag{6}$$

$$(1 + \xi\eta)F''' + \xi F'' + FF''/2 = (\xi/2)[F'(\partial F'/\partial\xi) - F''(\partial F/\partial\xi)]. \tag{7}$$

* Present address: Faculty of Mathematics, University of Cluj, R-3400 Cluj, CP 253, Romania.
† To whom the correspondence should be sent.

NOMENCLATURE

F	dimensionless streamfunction
g	acceleration due to gravity
K	permeability of the porous medium
L	length of the cylinder
q, Q	surface heat transfer and total surface heat transfer, respectively
r, x	radial and axial coordinates
r_0	radius of the cylinder
Ra_x	modified local Rayleigh number
T	temperature.

Greek symbols

α	equivalent thermal diffusivity
β	coefficient of thermal expansion
θ, μ	dimensionless temperature and viscosity of the fluid, respectively
ξ, η	transformed coordinates
ρ, ψ	density and dimensionless streamfunction, respectively.

Superscript

$'$	differentiation with respect to η.

Subscripts

cyl, fp	cylinder and flat plate, respectively
w, ∞	conditions at the wall and in the free stream, respectively

The boundary conditions (4) reduce to

$$F(\xi,0)=0, \quad F'(\xi,0)=1, \quad F'(\xi,\infty)=0. \tag{8}$$

3. SOLUTION

3.1. *Finite-difference method*

Equation (7) under conditions (8) has been solved numerically using a finite-difference scheme developed by Keller [3]. Since the method is described in great detail in refs. [3,4], it is not presented here. We have studied the effect of step sizes $\Delta\eta$ and $\Delta\xi$ and the edge of the boundary layer (η_∞) on the solution with a view to optimize them. Computations were carried out on a DEC-1090 computer with $\Delta\eta = 0.05$, $\Delta\xi = 0.1$ and $\eta_\infty = 8$. The results presented here are independent of the step sizes and η_∞ at least up to the fourth decimal place. The CPU time taken by a typical data is 6.1 s.

3.2. *Perturbation method*

Following the work by Aziz and Na [5], we assume a regular perturbation expansion for F in powers of small ξ as

$$F=\sum_{n=0}^{\infty} F_n(\eta)\xi^n. \tag{9}$$

Substituting (9) into equations (7) and (8), equating coefficients of like powers of ξ and truncating the expansion at the fifth term, we have

$$\xi^0: F_0'''+2^{-1}F_0F_0''=0 \tag{10}$$

$$\xi^1: F_1'''+2^{-1}(F_0F_1''-F_0'F_1'+2F_0''F_1)+\eta F_0'''+F_0''=0 \tag{11}$$

$$\xi^2: F_2'''+2^{-1}(F_0F_2''-2F_0'F_2'+3F_0''F_2)+\eta F_1'''+F_1''+F_1F_1''-2^{-1}(F_1')^2=0 \tag{12}$$

$$\xi^3: F_3'''+2^{-1}(F_0F_3''-3F_0'F_3'+4F_0''F_3)+\eta F_2'''+F_2''+F_1F_2''+3(F_1''F_2-F_1'F_2')/2=0 \tag{13}$$

$$\xi^4: F_4'''+2^{-1}(F_0F_4''-4F_0'F_4'+5F_0''F_4)+\eta F_3'''+F_3''+F_1F_3''+2F_1''F_3+3F_2F_2''/2-(F_2')^2-2F_1'F_3=0 \tag{14}$$

with the boundary conditions

$$F_0(0)=0, \quad F_0'(0)=1, \quad F_n(0)=F_n'(0)=0, \quad n=1,2,3,4 \tag{15}$$

$$F_n'(\infty)=0, \quad n=0,1,2,3,4.$$

We notice that the zeroth-order approximation given by equation (10) is similar to that obtained by Cheng and Minkowycz [7] in connection with the free convection along a vertical flat plate embedded in a saturated porous medium. The subsequent equations (11)–(14) involve linear simultaneous equations and are solved by using the finite-difference method mentioned earlier.

4. RESULTS AND DISCUSSION

First, we consider the heat transfer at the surface of the cylinder which is proportional to $[-F''(\xi,0)]$ and is given by

$$[-F''(\xi,0)]=-\left[\sum_{n=0}^{4} F_n''(0)\xi^n\right]. \tag{16}$$

As we have mentioned, equation (16) is valid for small values of ξ and cannot cover the range of ξ from 0 to 10 as reported in [1]. However, the convergence of the series (16) can be considerably improved if we use the Shanks [6] transformation. It is worth mentioning that this transformation is a remarkable scheme of nonlinear transformation to accelerate the convergence of some slowly convergent or even divergent series. This transformation is given as

$$e_k(S_n)=\frac{e_{k-1}(S_{n+1})e_{k-1}(S_{n-1})-e_{k-1}(S_n)^2}{e_{k-1}(S_{n+1})+e_{k-1}(S_{n-1})-2e_{k-1}(S_n)} \tag{17}$$

for $k = 1, 2, \ldots$ and $e_0(S_n) = S_n$, where S_n is the sum of the first n terms of the series and k is the number of iterations for which the Shanks transformation is applied. Applying this transformation to the series (16) we have compared the values of the heat transfer parameter $-F''(\xi,0)$ with those obtained by Minkowycz and Cheng [1] using the local nonsimilarity method. The comparison is given in Table 1. The heat transfer results $[-F''(\xi,0)]$ obtained by series solution using the Shanks transformation are found to be in good agreement with the finite-difference results for all values of ξ. The maximum difference is about 3% when $0 \leqslant \xi \leqslant 20$ and about 5% when $20 < \xi \leqslant 30$. However, the local nonsimilarity method is found to give satisfactory results only for $\xi \leqslant 1$ and in this case the maximum difference is about 4%. However, for $\xi > 1$, the results differ significantly from those of the finite-difference method and this difference increases with ξ. For example, at $\xi = 2$ the difference is about 11% and at $\xi = 10$ it is about 23%. The reason for this difference in the results when $\xi > 1$ is that in the local nonsimilarity method derivatives of certain terms with respect to ξ in the RHS of equation (10), which are not small for $\xi > 1$, are neglected causing significant error in the solution.

The ratio of the surface heat transfer along a vertical cylinder to that of a vertical flat plate embedded in the same porous medium is given by

$$q_{cyl}/q_{fp}=[-F''(\xi,0)]/[-F''(0)]. \tag{18}$$

Table 1. Comparison of surface heat transfer parameter $-F''(\xi,0)$

ξ	Finite-difference $-F''(\xi,0)$	Perturbation solution $-F''(\xi,0)$	Local non-similarity [1] $-F''(\xi,0)$
0.00	0.4438	0.4438	0.4438
0.25	0.4977	0.4957	0.4899
0.50	0.5472	0.5469	0.5332
0.75	0.5971	0.5975	0.5747
1.00	0.6479	0.6483	0.6149
1.50	0.7509	0.7495	—
2.00	0.8538	0.8499	0.7668
2.50	0.9562	0.9494	—
3.00	1.0576	1.0481	0.9085
4.00	1.2571	1.2427	1.044
5.00	1.4519	1.4337	1.176
6.00	1.6424	1.6211	1.305
7.00	1.8290	1.8050	1.435
8.00	2.0120	1.9856	1.565
9.00	2.1918	2.1629	1.696
10.00	2.3688	2.3368	1.830
12.00	2.7152	2.6753	
14.00	3.0531	3.0020	
16.00	3.3837	3.3173	
18.00	3.7080	3.6218	
20.00	4.0268	3.9161	
25.00	4.8031	4.6105	
30.00	5.5548	5.2511	

Table 2. Comparison of the ratio of surface heat transfer along a vertical cylinder to that of a vertical flat plate q_{cyl}/q_{fp}

ξ	Finite-difference q_{cyl}/q_{fp}	Perturbation solution q_{cyl}/q_{fp}	Local non-similarity [1] q_{cyl}/q_{fp}
0.00	1.0000	1.0000	1.000
0.25	1.1213	1.1137	—
0.50	1.2330	1.2287	1.202
0.75	1.3454	1.3424	—
1.00	1.4599	1.4566	1.386
1.50	1.6918	1.6839	1.561
2.00	1.9239	1.9095	1.727
2.50	2.1545	2.1332	1.889
3.00	2.3829	2.3549	2.044
4.00	2.8324	2.7922	2.351
5.00	3.2715	3.2213	2.645
6.00	3.7008	3.6424	2.941
7.00	4.1211	4.0557	3.236
8.00	4.5335	4.4613	3.530
9.00	4.9386	4.8594	3.821
10.00	5.3374	5.2503	4.110
12.00	6.1179	6.0110	
14.00	6.8793	6.7449	
16.00	7.6242	7.4533	
18.00	8.3550	8.1376	
20.00	9.0733	8.7989	
25.00	10.8225	10.3590	
30.00	12.5162	11.7984	

Using (16), this ratio can be written as

$$q_{cyl}/q_{fp} = 1 + \sum_{n=1}^{4} [F_n''(0)/(F_0''(0)]\xi^n$$
$$F''(0) = F_0''(0). \tag{19}$$

Applying the Shanks transformation to equation (19), we have calculated the ratio of the heat transfer q_{cyl}/q_{fp} which is presented in Table 2. The results of the present finite-difference technique and the local nonsimilarity method [1] are also given in Table 2. In this case also, the results of the series solution are found to be in good agreement with those of the finite-difference method, but the results of the local nonsimilarity method differ appreciably for large ξ ($\xi > 1$). The reason for this difference has already been explained.

Finally, we consider the ratio of total surface heat transfer for a vertical cylinder to that of a vertical flat plate with the same length embedded in a porous medium. From [1], we find that this ratio is given by

$$Q_{cyl}/Q_{fp} = [-F''(0)\xi_L]^{-1} \int_0^{\xi_L} [-F''(\xi,0)]\, d\xi \tag{20}$$

where ξ_L is defined by

$$\xi_L = 2\mu\alpha L/[r_0\rho_\infty g\beta K(T_w - T_\infty)]. \tag{21}$$

Using equation (16), the ratio of the total surface heat transfer can be expressed as

$$Q_{cyl}/Q_{fp} = 1 + \sum_{n=0}^{4} (n+1)^{-1}\xi_L^n F_n''(0)/F_0''(0). \tag{22}$$

The results of equation (20) obtained by the finite-difference scheme and of (22) by applying the Shanks transformation are shown in Table 3. It is found that the results of the series solution using the transformation are in good agreement with those of the finite-difference method. We have also compared our finite-difference results (Q_{cyl}/Q_{fp}) with those of the local nonsimilarity method [1] and the comparison is given in Fig. 1. As expected the results are found to differ appreciably for large ξ_L($\xi_L > 1$).

Table 3. Comparison of the ratio of total surface heat transfer along a vertical cylinder to that of a vertical flat plate Q_{cyl}/Q_{fp}

ξ	Finite-difference Q_{cyl}/Q_{fp}	Perturbation solution Q_{cyl}/Q_{fp}
0.00	1.000	1.000
0.25	1.0621	1.0568
0.50	1.1197	1.1139
0.75	1.1761	1.1709
1.00	1.2327	1.2281
1.50	1.3470	1.3424
2.00	1.4623	1.4564
2.50	1.5777	1.5700
3.00	1.6929	1.6833
4.00	1.9218	1.9086
5.00	2.1480	2.1321
6.00	2.3712	2.3539
7.00	2.5912	2.5740
8.00	2.8083	2.7923
9.00	3.0226	3.0089
10.00	3.2342	3.2237
12.00	3.6500	3.6484
14.00	4.0572	4.0665
16.00	4.4567	4.4780
18.00	4.8493	4.8832
20.00	5.2359	5.8222
25.00	6.1793	6.2534
30.00	7.0950	7.1888

5. CONCLUSIONS

The results obtained by the perturbation method with Shanks transformation are found to be in good agreement with those of the finite-difference scheme for all values of ξ, whereas the results of the local nonsimilarity method are in good agreement with those of the finite-difference scheme only for small ξ ($\xi < 1$), but for large ξ ($\xi > 1$) they differ

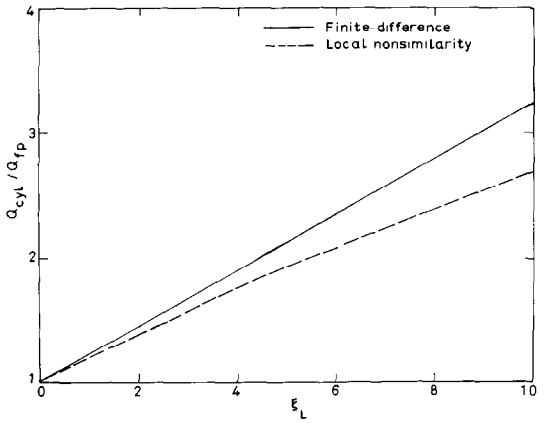

FIG. 1. Comparison of total heat-transfer ratio Q_{cyl}/Q_{fp}.

appreciably. Therefore, the local nonsimilarity method is not suitable for those nonsimilar problems where the nonsimilar terms are not small. However, the perturbation method with the Shanks transformation can successfully be used to tackle nonsimilar problems with relatively fair degree of accuracy.

REFERENCES

1. W. J. Minkowycz and P. Cheng, Free convection about a vertical cylinder embedded in a porous medium, *Int. J. Heat Mass Transfer* **19**, 805–813 (1976).
2. E. M. Sparrow, H. Quack and C. J. Boerner, Local nonsimilarity boundary-layer solutions, *AIAA Jl.* **8**, 1936–1942 (1970).
3. H. B. Keller, A new difference scheme for parabolic problems. In *Numerical Solution of Partial Differential Equations* (Edited by J. Bramble), Vol. II. Academic Press, New York (1970).
4. H. B. Keller and T. Cebeci, Accurate numerical methods in boundary layers—I. Two-dimensional laminar flows, *Proc. 2nd Int. Conference on Numerical Methods in Fluid Dynamics, Lecture Notes in Physics*, Vol. 8. Springer, New York (1971).
5. A. Aziz and T. Y. Na, Improved perturbation solutions for laminar natural convection on a vertical cylinder, *Wärme- u. Stoff übertr.* **16**, 83–87 (1982).
6. D. Shanks, Nonlinear transformation of divergent and slowly convergent sequences, *J. Math. Phys.* **34**, 1–42 (1955).
7. P. Cheng and W. J. Minkowycz, Free convection about a vertical flat plate embedded in a porous medium with application to heat transfer from a dyke, *J. geophys. Res.* **82**, 2040–2044 (1977).

Int. J. Heat Mass Transfer. Vol. 28, No. 11, pp. 2174–2176, 1985
Printed in Great Britain

0017-9310/85 $3.00 + 0.00

Pressure/temperature ignition limits of fuel droplet vaporizing over a hot plate

P. CHO and C. K. LAW
Department of Mechanical Engineering, University of California, Davis, CA 95616, U.S.A.

(*Received* 25 *February* 1985 *and in final form* 17 *June* 1985)

1. INTRODUCTION

IN VARIOUS forms of liquid-fuelled combustors part of the injected fuel may impinge on the hot walls of the combustion chamber either intentionally or by design. A particularly innovative example is the recent development of the open chamber, stratified charge engines in which the fuel is directly injected into a hollowed space in the piston head. It is suggested that this design facilitates ignition of the fuel spray through its interaction with the hot surface, and thereby results in the observed improvement in the engine performance in terms of combustion efficiency and pollutant emissions.

The scientific problem of interest here is the ignition of a fuel droplet over a hot plate. In order to appreciate the complexity and richness of the phenomena of interest, let us first consider the basic process of droplet gasification over a hot plate, which is commonly known as the Leidenfrost phenomenon [1, 2]. Figure 1, obtained in the course of present study, shows the droplet evaporation time τ of a dodecane droplet as a function of the plate temperature T_w for three chamber pressures; the initial droplet diameter is about 2 mm. It is seen that the lifetime curve consists of three segments, namely a low-temperature regime during which the droplet is in full contact with the surface and τ decreases rapidly with increasing T_w, a transition regime during which the droplet begins to push itself off the plate with increasing vapor pressure and τ increases with T_w, and a third regime during which the droplet is fully levitated by its vapor pressure and τ again decreases with T_w, albeit slowly. The minimum and maximum points are respectively known as the nucleate boiling point and the Leidenfrost point.

Figure 1 further shows that with increasing pressure the vaporization time curves are shifted in the direction of higher

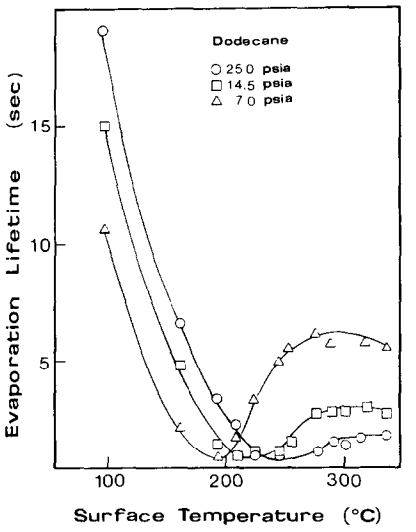

FIG. 1. Effect of ambient pressure and plate temperature on droplet evaporation lifetime.